



## Integrative analysis reveals chemokines CCL2 and CXCL5 mediated shear stress-induced aortic dissection formation

Chao Xue<sup>a,1</sup>, Liqing Jiang<sup>a,1</sup>, Bin Zhang<sup>a,1</sup>, Jingwei Sun<sup>a</sup>, Hanzhao Zhu<sup>a</sup>, Linhe Lu<sup>a</sup>, Liyun Zhang<sup>a</sup>, Bo Yu<sup>a</sup>, Weiguang Wang<sup>a</sup>, Bo Xu<sup>a</sup>, Zhenxiao Jin<sup>a</sup>, Shiqiang Yu<sup>a</sup>, Jincheng Liu<sup>a,\*\*</sup>, Kai Ren<sup>a,\*\*\*</sup>, Weixun Duan<sup>a,\*</sup>

<sup>a</sup> Department of Cardiovascular Surgery, Xijing Hospital, The Fourth Military Medical University, Xi'an, China

### A B S T R A C T

**Background:** Aortic dissection (AD) is a critical emergency in cardiovascular disease. AD occurs only in specific sites of the aorta, and the variation of shear stress in different aortic segments is a possible cause not reported. This study investigated the key molecules involved in shear stress-induced AD through quantitative bioinformatic analysis of a public RNA sequencing database and clinical tissue sample validation.

**Methods:** Gene expression data from the GSE153434, GSE147026, and GSE52093 datasets were downloaded from the Gene Expression Omnibus. Next, differently expressed genes (DEGs) in each dataset were identified and integrated to identify common AD DEGs. STRING, Cytoscape, and MCODE were used to identify hub genes and crucial clustering modules, and Connectivity Map (CMap) was used to identify positive and negative agents. The same procedure was performed for the GSE160611 dataset to obtain shear stress-induced human aortic endothelial cell (HAEC) DEGs. After the integration of these two DEGs sets to identify shear stress-associated hub DEGs in AD, Gene Ontology Enrichment Analysis was performed. The common chemokine receptors and ligands in AD were identified by analyzing AD's three RNA sequencing datasets. Their origin was verified by analyzing AD single-cell sequencing data and validated by immunoblotting and immunofluorescence.

**Results:** We identified 100 down-regulated and 50 up-regulated AD common DEGs. Enrichment results showed that common DEGs were closely related to blood vessel morphogenesis, muscle structure development, muscle tissue development, and chemotaxis. Among those DEGs, MYC, CCL2, and SPP1 are the three molecules with the highest degree. A crucial cluster of 15 genes was identified using MCODE, which contained inflammation-related genes with elevated expression and muscle cell-related genes with decreased expression, and CCL2 is central to immune-related genes. CMap confirmed MEK inhibitors and ALK inhibitors as possible therapeutic agents for AD. Moreover, 366 shear stress-associated DEGs in HAEC were identified in the GSE160611 dataset. After taking the intersection, we identified five shear stress-associated hub DEGs in AD (ANGPTL4, SNAI2, CCL2, GADD45B, and PROM1), and the enrichment analysis indicated they were related to the endothelial cell apoptotic process. Chemokine CCL2 was the molecule with a high degree in both DEG sets. Besides CCL2, CXCL5 was the only chemokine ligand differentially expressed in the three datasets. Additionally, immunoblotting confirmed the increased expression of CCL2 and CXCL5 in clinical tissue samples. Further research at the single-cell level revealed that CCL2 has multiple origins, and CXCL5 is macrophage-derived.

**Conclusion:** Through integrative analysis, we identified core common AD DEGs and possible therapeutic agents based on these DEGs. We elucidated that the chemokine CCL2 and CXCL5-mediated "Endothelial-Monocyte-Neutrophil" axis may contribute to the development of shear stress-induced AD. These findings provide possible therapeutic targets for the prevention and treatment of AD.

\* Corresponding author.

\*\* Corresponding author.

\*\*\* Corresponding author.

E-mail addresses: [liujcxjyy@163.com](mailto:liujcxjyy@163.com) (J. Liu), [rk90108@163.com](mailto:rk90108@163.com) (K. Ren), [duanweixun@126.com](mailto:duanweixun@126.com) (W. Duan).

<sup>1</sup> These authors contributed equally to this work and shared the first authorship.

<https://doi.org/10.1016/j.heliyon.2023.e23312>

Received 23 May 2023; Received in revised form 23 November 2023; Accepted 30 November 2023

Available online 4 December 2023

2405-8440/© 2023 The Authors. Published by Elsevier Ltd. This is an open access article under the CC BY-NC-ND license (<http://creativecommons.org/licenses/by-nc-nd/4.0/>).

## 1. Background

Aortic dissection (AD) is a condition in which blood flows into the medium of the aorta through an intimal tear, forcing the intima and adventitia to separate and predispose the patient to death due to rupture of the aorta. Additionally, AD could occur from a longitudinal dissection tear along the aorta, causing ischemia of vital organs. The mortality rate increases by 1 %–2 % for every hour that passes once AD occurs, resulting in a 48 h mortality rate of approximately 50 % without timely surgical intervention [1]. Therefore, preventing this disease's recurrence and initiating aggressive treatment after its onset is essential. Understanding its pathogenesis is the basis for prevention. Recently, much work has been done on the pathogenesis of AD, and medium degeneration has been confirmed as a key pathophysiological feature.

Vascular smooth muscle cells (VSMCs) are the predominant cell type within the aortic media, and researchers have proposed underlying mechanisms for the loss [2], apoptosis [3], and phenotypic switching [4] of VSMCs involved in the development of AD. Besides VSMC disorders, extracellular matrix (ECM) abnormalities are critical pathophysiological features of AD. ECM abnormalities and susceptibility to AD arise when mutations are present in genes encoding relevant ECM components, such as FBN1, which encodes fibrillin-1 in Marfan syndromes, or collagen fibrillin-related genes, such as COL5A1, COL5A2, TNXB, COL3A1, PLOD1, COL1A1, and COL1A2 in Ehlers–Danlos syndrome. Additionally, immune-related cells, such as macrophages, are involved in the pathogenesis of AD [5].

Although these studies have provided insight into the pathogenesis of AD, there was an under-recognized problem, which was why AD occurs only in specific aortic segments, given that all segments share the same genetic background. The aorta receives high-velocity blood flow and is exposed to complex and highly variable shear stress. In addition, the tear locations of aortic dissections were highly coincident with the area of maximum elevation of shear stress [6]. Therefore, focusing on the role of shear stress in this process may help solve this problem. Hypertension contributes significantly to increased shear stress on the aorta and is also a critical risk factor for aortic dissection. However, the increased incidence of AD attributed to hypertension is not merely due to increased shear stress, which exceeds the stiffness of the aorta. Because, as well as being agents that increase blood pressure, the combination of Angiotensin II (ANG II) increases the incidence of AD in the animal model of AD constructed using BAPN. However, the same effect is yet to be achieved with norepinephrine, another clinically frequently used vasopressor [7]. Thus, shear stress-induced molecular alterations may be the key to their involvement in AD, and revealing the molecular changes associated with shear stress in the aorta is a crucial step in uncovering the pathogenesis of AD. In this study, we conducted bioinformatic analyses of human AD aorta transcriptome sequencing data, shear stress-induced human aortic endothelial cell (HAEC) (which is the cell of the aorta directly exposed to the blood flow and shear stress) change transcriptome sequencing data, human AD aorta scRNA-sequencing data in a public database, and validation of clinical tissue specimens to investigate the common hub genes that will help elucidate the potential mechanisms of shear stress-induced AD and identify the potential therapeutic agents.

## 2. Methods

### 2.1. Study design and data collection

All eligible datasets were downloaded from the Gene Expression Omnibus (GEO) database. Next, we searched for related gene expression data using keywords: AD, shear stress, and human aorta. The selection criteria were: 1) AD arrays containing at least  $\geq 4$  samples in the normal and patient groups, and the included test specimens were from adult humans, 2) shear stress-related arrays from human aortic cells, and 3) gene expression profiling using an array. Based on these selection criteria, we eventually included three AD datasets: GSE147206 [8], GSE153434 [9], and GSE52093 [10]. The sample size, demographic, and clinical characteristics of these data sets are shown in Table 1. Additionally, we selected the GSE160611 dataset - an expression profile of shear stress-induced HAEC transcriptome sequencing data. Lastly, for human AD scRNA sequencing data, we selected the GSE213740 dataset [11].

**Table 1**

The sample size, demographic and clinical characteristics of these AD data sets.

	GSE153434		GSE147026		GSE52093	
	Control Cohort	Experiment Cohort	Control Cohort	Experiment Cohort	Control Cohort	Experiment Cohort
Source and size of tissue sample	(n = 10) Normal ascending aortic tissue samples from patients undergoing coronary artery bypass grafting surgery (CABG) without any aortic diseases	(n = 10) The TAAD ascending aorta sample from patients undergoing surgery	(n = 4) Normal aortic tissue from heart transplantation donor due to cerebrovascular or motor vehicle accident death	(n = 4) Samples with acute ascending aortic dissection from patients undergoing surgery	(n = 5) Normal aorta from organ donors	(n = 7) Dissected ascending aorta specimens were obtained through operation
Age	60.9 ± 3.0	59.3 ± 3.9	48.0 ± 5.2	54.3 ± 3.9	38.6 ± 4.8	42.0 ± 17.0
Male(%)	4 (40 %)	5 (50 %)	2 (50 %)	2 (50 %)	5(100 %)	6(85.7 %)
Smoking	0(0 %)	0(0 %)	1(25 %)	1(25 %)	2(40 %)	2(28.6 %)
Hypertension	3(30 %)	7(70 %)	1(25 %)	4(100 %)	2(40 %)	6(85.7 %)
Diabete	0(0 %)	1(10 %)	0(0 %)	0(0 %)	0(0 %)	1(14.3 %)
Alcoholic	0(0 %)	0(0 %)	0(0 %)	0(0 %)	NA	NA

## 2.2. Analysis of differential expression genes

The raw expression datasets were downloaded and processed using log<sub>2</sub> transformation in R language. Additionally, differently expressed genes (DEGs) were identified using the R "limma" package with the threshold of adjusted P-value < 0.05 and |log fold change| ≥ 1. Lastly, the online Venn diagram tool (<http://bioinformatics.psb.ugent.be/webtools/Venn/>) was used to obtain the common DEGs.

## 2.3. Gene Ontology and Kyoto Encyclopedia of Genes and Genomes pathway enrichment analyses

The Metascape database (<https://metascape.org/gp/index.htm>) was used to import the targets of common AD DEG for Kyoto Encyclopedia of Genes and Genomes (KEGG) pathway enrichment and Gene Ontology (GO) functional analyses [12]. Next, GO and KEGG pathway enrichment analyses were performed for the featured genes obtained by the principal component analysis (PCA) algorithm using "clusterProfiler," "org.Hs.eg.db," and "enrich plot" packages in R. Terms were considered significantly enriched with P < 0.05 and q < 1. Lastly, a Goplot was used to visualize the combination of DEG enrichment results [13].

## 2.4. Protein-protein interaction network construction of differently expressed genes

Protein-protein interaction (PPI) networks of common AD and HAEC shear stress-induced DEGs were constructed using the STRING website (<https://cn.string-db.org/>). Next, the reconstruction was performed using Cytoscape version 3.6.1 and further analyzed using Molecular Complex Detection (MCODE).

## 2.5. Identification of candidate small molecule compounds by Connectivity Map

The Connectivity Map [14], or CMap, is a tool that leverages cellular reactions to perturbation to identify connections between disorders, genes, and therapeutics. It could be used to anticipate prospective small molecules that impact the phenotype brought on by a specific gene expression. The 150 previously mentioned common AD DEG were split into two groups (upregulation and down-regulation) and then submitted to the CMap database to investigate prospective small molecule medicines that may treat AD. A high connectivity score predicts that small molecule agents may cause the same genetic modulation as the disorder. A low connectivity score suggests that small compounds may help treat disease by reversing gene expression.

## 2.6. Analysis of immune cell characteristics

Normalized AD expression data were analyzed using CIBERSORTx to predict the proportion of 22 types of immune cells in each tissue, and the LM22 gene expression profile was used as reference [15].

## 2.7. scRNA-sequencing data processing and clustering

We used the R package Seurat (version 3.1.2) for scRNA-sequencing data processing and clustering [16]. Six single-cell data were integrated using the harmony package (<https://github.com/immunogenomics/harmony>) to control batch effects when integrating data from different samples. Poor-quality cells were excluded based on the following quality control criteria: >200 genes per cell, <30 % mitochondrial genes, and the absence of the hemoglobin subunit beta gene. The Seurat manual instructions were followed, and the actions were as follows: the most variable genes (2000 genes) for all samples were used for linear dimensional reduction (PCA). Additionally, the Seurat "FindCluster" function (resolution = 0.5) was used for cluster analysis, which is based on plotting the clustering tree in Fig. S1 (<https://lazappi.github.io/clustree>), and Uniform Manifold Approximation and Projection (UMAP) was used for nonlinear dimensional reduction to visualize the results in UMAP plots. Lastly, using default options, Seurat's "FindAllMarkers" tool was used to identify conserved (marker) genes in the clusters, and cell annotation was conducted.

## 2.8. Immunoblotting

The appropriate volume of lysate buffer containing protease and phosphatase inhibitors was added according to the mass and volume of the aortic sample obtained from the patient with aortic dissection during the surgery and then placed on ice for 5 min. Centrifuge at 12,000 rpm for 10 min at 4 °C in a cryogenic freezing centrifuge, separating the supernatant as the resulting protein extract. A BCA protein quantification kit quantified protein concentrations. The protein samples were diluted with 5 × Loading Buffer and PBS, boiled in a boiling water bath for 5 min, and made into a loading solution for preparation. The loading volume for this experiment was 20 µl, containing 40 µg of protein. And lysates were separated by SDS-PAGE and transferred to PVDF membranes. After being blocked with non-fat milk, membranes were probed with the CLL2(Wanleibio, WL02966), CXCL5(Affinity, DF9919), and β-actin (wanleibio, WL01372) primary antibody and secondary IgG-HRP antibody (Wanleibio, WLA023), and the bands were visualized with ECL chromogenic solution (Wanleibio, WLA003) and developed with Kodak film. The images were analyzed using Quantity One software (Bio-Rad Laboratories, Inc.).

### 2.9. Immunofluorescence staining

After deparaffinized, rehydrating, antigen retrieval, and endogenous peroxidase blocking, sections were blocked with 10 % donkey serum. The first MPO primary antibody (Servicebio, GB11224) was incubated, followed by a secondary antibody marked with HRP (Servicebio, GB21303), and then CY3-TSA solution (Servicebio, G1223). After microwave treatment, incubation continued as above with a second CD68 primary antibody (Servicebio, GB113150), corresponding to the HRP-labelled secondary antibody (Servicebio, GB23303) and FITC-TSA (Servicebio, G1222). The procedure is then repeated for the microwave treatment and a third CXCL5 primary antibody (Abcam, Ab305100), corresponding to the CY5-labelled secondary antibody (Servicebio, GB27303). The sections were washed three times with TBST for 5 min before each incubation during the above process. Finally, incubate slides with DAPI for 10 min at room temperature, incubate slides with spontaneous fluorescence quenching reagent for 5 min, then wash slides under flowing water for 10 min. Coverslip with anti-fade mounting medium after washing three times for 5 min. Images were obtained using the Slice scanner (panoramic; MIDI:3Dhitech). DAPI glows blue by UV excitation wavelength 330–380 nm and emission wavelength 420 nm; FITC glows green by excitation wavelength 465–495 nm and emission wavelength 515–555 nm; CY3 glows red by excitation

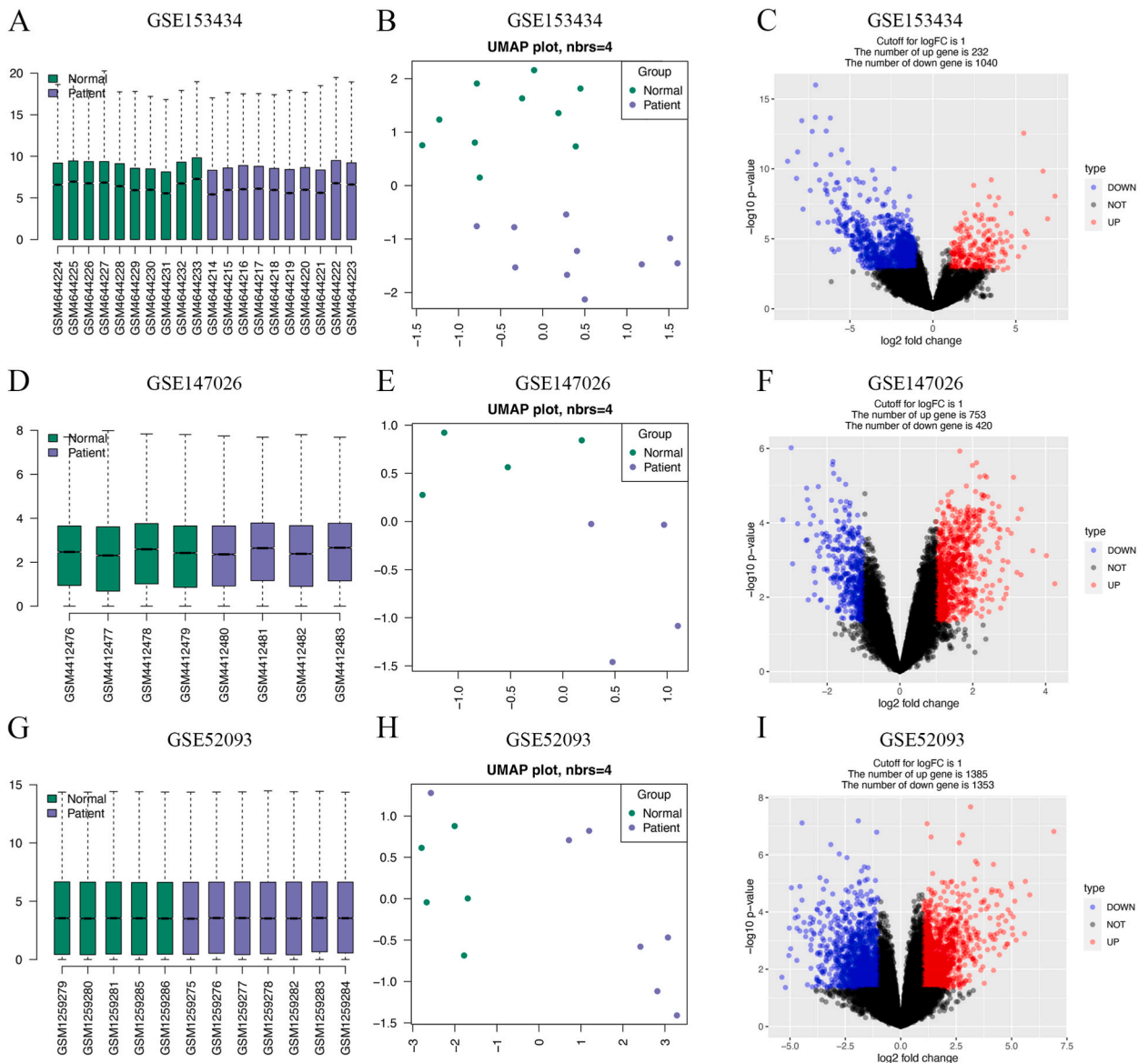


**Fig. 1.** Quality control of aortic dissection transcriptome datasets and identification of DEGs. (A) Normalized data of GSE153434. (B) UMAP of GSE153434. (C) Volcano plots of DEGs from GSE153434. (D) Normalized data of GSE147026. (E) UMAP of GSE147026. (F) Volcano plots of DEGs from GSE147026. (G) Normalized data of GSE52093. (H) UMAP of GSE52093. (I) Volcano plots of DEGs from GSE52093. UMAP: uniform manifold approximation and projection. DEGs: differentially expressed genes.



wavelength 510–560 nm and emission wavelength 590 nm. CY5 glows pink by excitation wavelength 608–648 nm and emission wavelength 672–712 nm.

### 3. Result

#### 3.1. Identification of common aorta dissection DEGs

The boxplot in Fig. 1 shows the consistency of the samples (Fig. 1A, D, and 1G), and the proportions of normal and AD patient groups showed individual PCA differences (Fig. 1B, E, and 1H). Moreover, 1272 DEGs (232 up-regulated and 1040 down-regulated) were identified in AD patients and normal individuals using the edgeR package in the GSE153434 dataset (Fig. 1C). Additionally, 1173 DEGs (753 up-regulated and 420 down-regulated) were screened in the GSE147026 dataset (Fig. 1F), and 2738 (1385 up-regulated and 1253 down-regulated) in the GSE 52093 dataset (Fig. 1I). Next, common up-regulated and down-regulated DEGs were separately

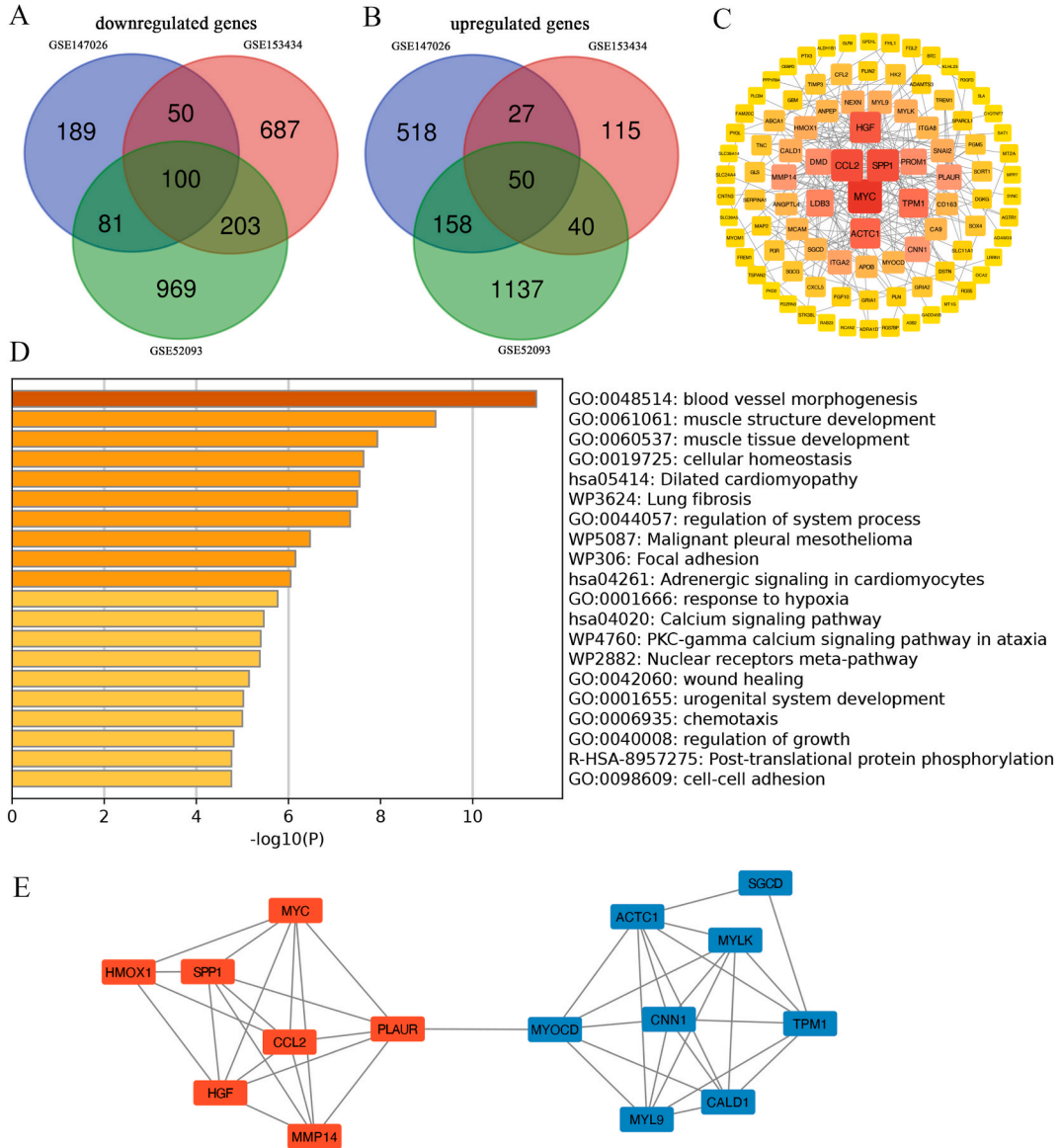


**Fig. 2.** Identification, PPI network construction, and enrichment analysis of the core DEGs of AD. (A) A total of 100 genes with common down-regulated expressions were found in the three datasets. (B) A total of 50 genes with common up-regulated expression in the three datasets. (C) PPI network constructed with the core DEGs. The darker the color, the higher the connectivity of genes. (D) Enrichment of the core DEGs in Metascape. (E) A crucial clustering module, including 15 nodes and 42 edges, was defined by MCODE. DEGs: differently expressed genes. PPI: protein-protein interaction. MCODE: Molecular Complex Detection.

identified after the intersection of the Venn diagrams (Fig. 1C). Lastly, 100 commonly down-regulated genes (Fig. 2A) and 50 commonly up-regulated genes (Fig. 2B) were identified.

Subsequently, the targets of common AD DEG were imported from the Metascape database (<https://metascape.org/gp/index.htm>) for KEGG pathway enrichment and GO functional analyses, which showed that common DEGs were closely related to blood vessel morphogenesis, muscle structure development, muscle tissue development, and chemotaxis (Fig. 2D). Furthermore, the PPI network of the DEGs was screened and visualized using STRING and Cytoscape, respectively, to reveal the potential relationships between proteins encoded by common DEGs and identify hub genes. The nodes were colored according to their degree (Fig. 2C); MYC, CCL2, and SPP1 molecules had the highest degrees. Next, MCODE, a plug-in of Cytoscape, was used to conduct module analysis to detect crucial clustering modules. A module with 15 nodes and 42 edges with a cluster score (density times the number of members) of 6 (Fig. 2E) was defined. The nodes were colored according to the type of up-regulation or down-regulation of nodes of crucial clustering modules. The up-regulated genes are shown in red, and the down-regulated genes in blue (Fig. 2E). The down-regulated genes, including ACTC1, CALD1, MYL9, and MYOCD, were involved in muscle cell-related pathophysiological processes, and up-regulated genes, including CCL2 and SPP1, were related to the inflammatory response. These results are consistent with the enrichment analysis in Metascape, suggesting that increased inflammation and down-regulation of smooth muscle cell-related molecules are hallmark characteristics of AD, and CCL2 is central to immune-related genes. Next, the common AD DEGs obtained above were used to investigate potential therapeutic agents for AD by the Query tool from the Cmap online platform. Top10 positive drugs, and top10 negative drugs, mechanism of activities (MOA), and target were shown in Fig. 3A, blue means negative while red means positive. Their normalized connectivity scores are visualized in Fig. 3B. Negative agents mainly include MEK inhibitors and ALK inhibitors.

### 3.2. Identification of shear stress-associated hub differentially expressed genes in aortic dissection

Considering that shear stress may be involved in the occurrence and development of AD, we explored the underlying mechanism by analyzing the GSE160611 dataset, which revealed the effect of shear stress on gene expression in HAEC. Notably, endothelial cells

A

name	moa	target_name
CEP-37440	ALK inhibitor	ALK
dolasetron	Serotonin receptor antagonist	HTR3A
BRD-K26619122	GABA receptor antagonist	GABRA1 GABRB2 GABRG2 GLRA1 GLRB
TAK-733	MEK inhibitor	MAP2K1
AS-703026	MEK inhibitor	MAP2K1 MAP2K2
phenoxybenzamine	Adrenergic receptor antagonist	ADRA2B ADRA1A ADRA1B ADRA1D ADRA2A ADRA2C ADRB2 CALM1
AZ-628	RAF inhibitor	BRAF RAF1
ilomastat	Matrix metalloprotease inhibitor	ACAN ADAM28 MMP1 MMP12 MMP13 MMP14 MMP2 MMP3 MMP8 MMP9
GW-788388	ALK inhibitor	TGFBR1 LCK MAPK14
pyrazolanthrone	JNK inhibitor	MAPK10 MAPK8 MAPK9 TTK LRRK2 MAPK8IP1
mefloquine	Adenosine receptor antagonist	PANX1 ADORA2A HBA1
MRS-1220	Hemoglobin antagonist	ADORA3 ADORA2B
allectinib	Adenosine receptor antagonist	ALK MET
GSK-461364	ALK inhibitor	PLK1
dexketoprofen	PLK inhibitor	PTGS2 PTGS1
INCA-6	Cyclooxygenase inhibitor	NFATC1
penfluridol	Calcineurin inhibitor	DRD1 DRD2 CACNA1G
capsaicin	Calcium channel blocker	TRPV1 ENOX2 CFTR
BRD-K72783841	TRPV agonist	EGFR
ingenol-mebutate	EGFR inhibitor	PRKCD PRKCA PRKCB PRKCE PRKCG
	PKC activator	

B

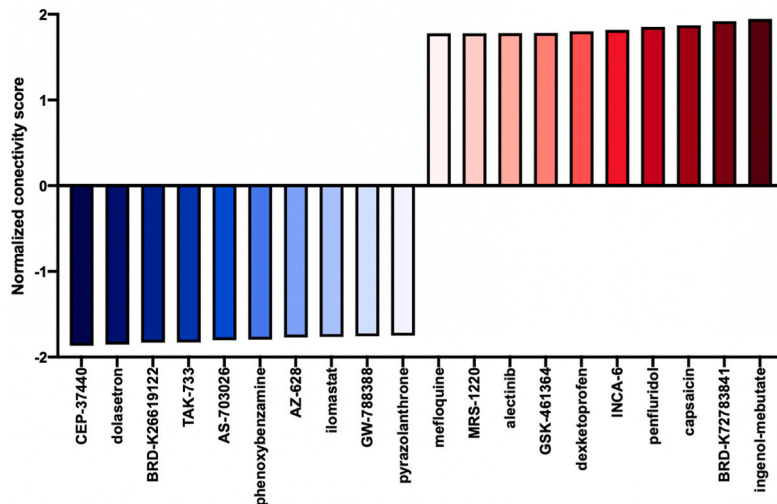
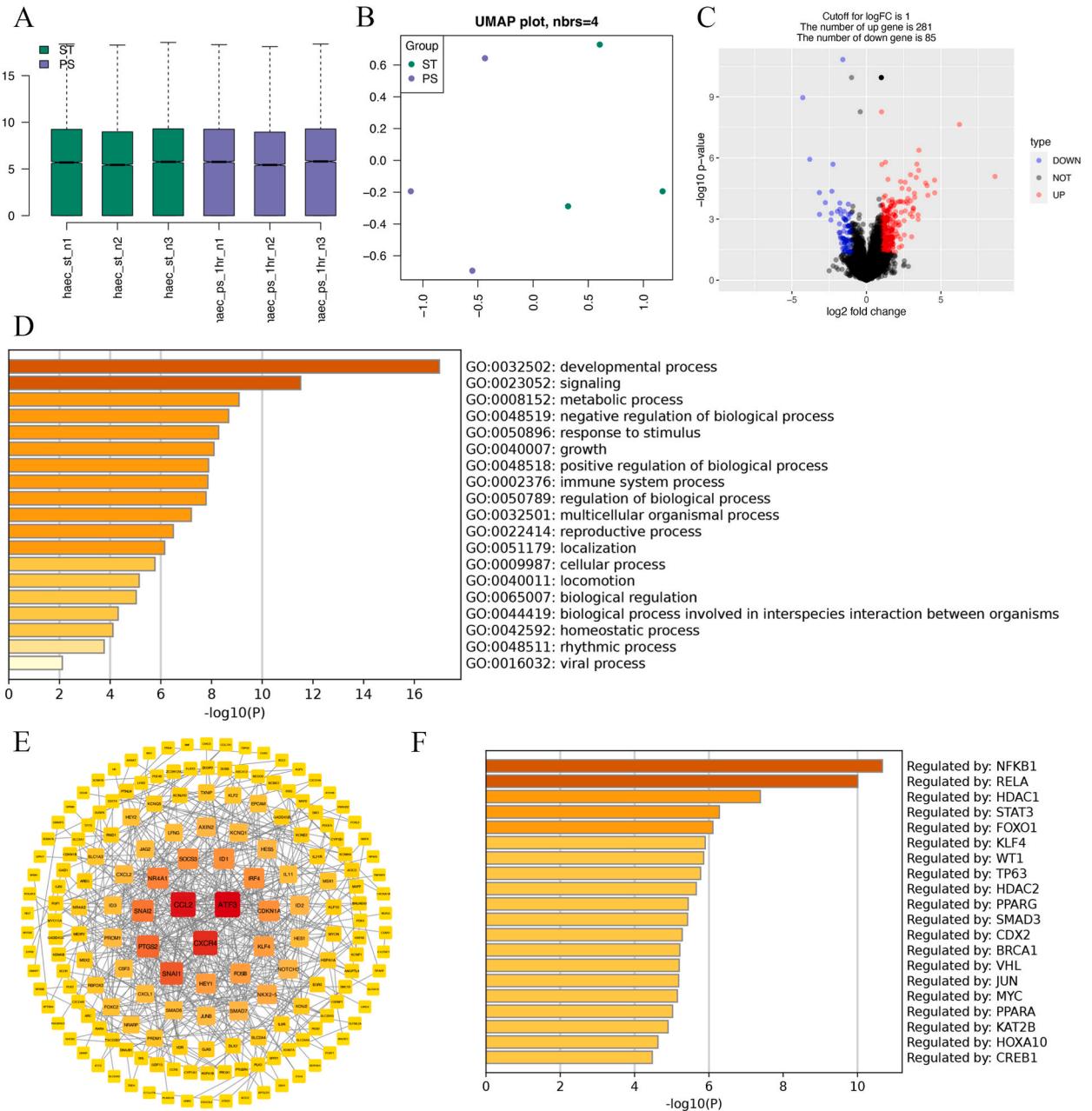


Fig. 3. Potential therapeutic agents for AD by the Query tool from the Cmap online platform. (A) Top10 positive and top10 negative drugs, mechanism of activities (MOA), blue means negative, and red represents positive. (B) Normalized connectivity scores of potential agents.

likely show an adaptive capacity to shear stress, meaning that the biological effects of shear stress gradually disappear over time [17]. Therefore, we chose HAEC expression data at a steady state and after administration of shear stress for 1 h. Regarding the stress type, pulsatile shear was selected because of its prevalence in straight segments of arteries, and oscillatory shear was observed at branch points [18]. Moreover, the boxplot shows the consistency of the sample, and the proportions of steady-state and pulsatile shear showed individual PCA differences (Fig. 4A). We identified 366 DEGs (281 up-regulated and 85 down-regulated)(Fig. 4C). The top-level GO biological processes in the Metascape enrichment analysis are closely related to developmental processes, signaling, metabolic, negative regulation of biological process, and response to stimulus, which were shown in Fig. 4D.

The PPI network of the DEGs was screened and visualized using STRING and Cytoscape, respectively. The nodes were colored according to their degrees, and CCL2, CXCR4, and ATF3 molecules showed the highest degrees(Fig. 4E). Enrichment analysis in



**Fig. 4.** Identification, PPI network construction, and enrichment analysis of the shear stress-induced HAEC DEGs. (A) Normalized data of GSE160611. (B) UMAP of GSE160611. (C) Volcano plots of DEGs from GSE160611. (D) Enrichment of the DEGs in Metascape. (E) PPI network constructed with the core DEGs. The darker the color, the higher the connectivity of genes. (F) The possibly influenced transcription factors revealed by enrichment analysis in TTRUST. DEGs: differently expressed genes. HAEC: human aortic endothelial cell. PPI: protein-protein interaction.

TTRUST revealed that NFKB1 and RELA were the possibly influenced transcription factors (Fig. 4F). Additionally, CCL2 was the core DEG in both datasets, suggesting that chemokines are critical for shear stress-induced AD. Furthermore, shear stress-induced DEGs were intersected with the common DEGs of AD to obtain shear stress-associated hub genes in AD. We identified one down-regulated (PROM1) and four up-regulated genes (ANGPTL4, SNAI2, CCL2, and GADD45B) (Fig. 5A and B). Enrichment of these five genes suggests their relationship to endothelial cell apoptosis (Fig. 5C). Therefore, we hypothesized that shear stress could lead to endothelial cell apoptosis and CCL2 release, recruiting monocytes to local adhesions - this is a possible mechanism for its involvement in AD development. Further analysis of the changes in other relevant chemokine ligands and receptors in HAEC exposed to shear stress suggested increased CCL2 expression and decreased CXCL1, CXCL2, and CXCR4 expressions in HAEC at 1 h. Moreover, at 4 h, CCL2 expression decreased, and the expression level was lower than the basal expression; at 24 h, a further decline was observed (Fig. 6A–C). This is consistent with previous results showing that the aortic endothelium exhibits a certain degree of adaptation to shear stress.

3.3. Chemokine ligand and receptor in aortic dissection

As described above, we established the vital role of chemokine CCL2 in AD. Is it possible that other chemokines are also involved in AD development? Therefore, we analyzed chemokine-related ligands and receptors in the three AD datasets. CCL2, CCL3, CCL7, CCL20, CCL21, CXCL3, CXCL5, CXCL14, and CX3CR1 showed significantly different expression levels in GSE153434 (Fig. 6D). Moreover, CCL2, CCL5, CCL8, CCL18, CXCL1, CXCL2, CXCL5, CXCL8, CXCL9, CXCL12, CXCL16, CCR1, CCR2, CCR5 and CXCR4 were differentially expressed in the GSE147026 dataset (Fig. 6E); CCL2, CCL5, CCL7, CCL14, CCL15, CCL27, CXCL1, and CXCL5 were differentially expressed in the GSE52093 data set. Therefore, among all chemokine ligands and receptors (Fig. 6F), CCL2 and CXCL5 were the differently expressed chemokine ligands common to all three datasets. Next, we performed immunoblotting of human tissue samples to verify the differential expression of these two molecules at the protein level, and the details of the clinical tissue samples are shown in Table 2. CCL2 and CXCL5 levels were significantly elevated in tissue samples of AD patients (Fig. 6G–J). Since chemokines are involved in the induction of immune cell infiltration, we believe that CCL2 and CXCL5-mediated immune cell infiltration is an

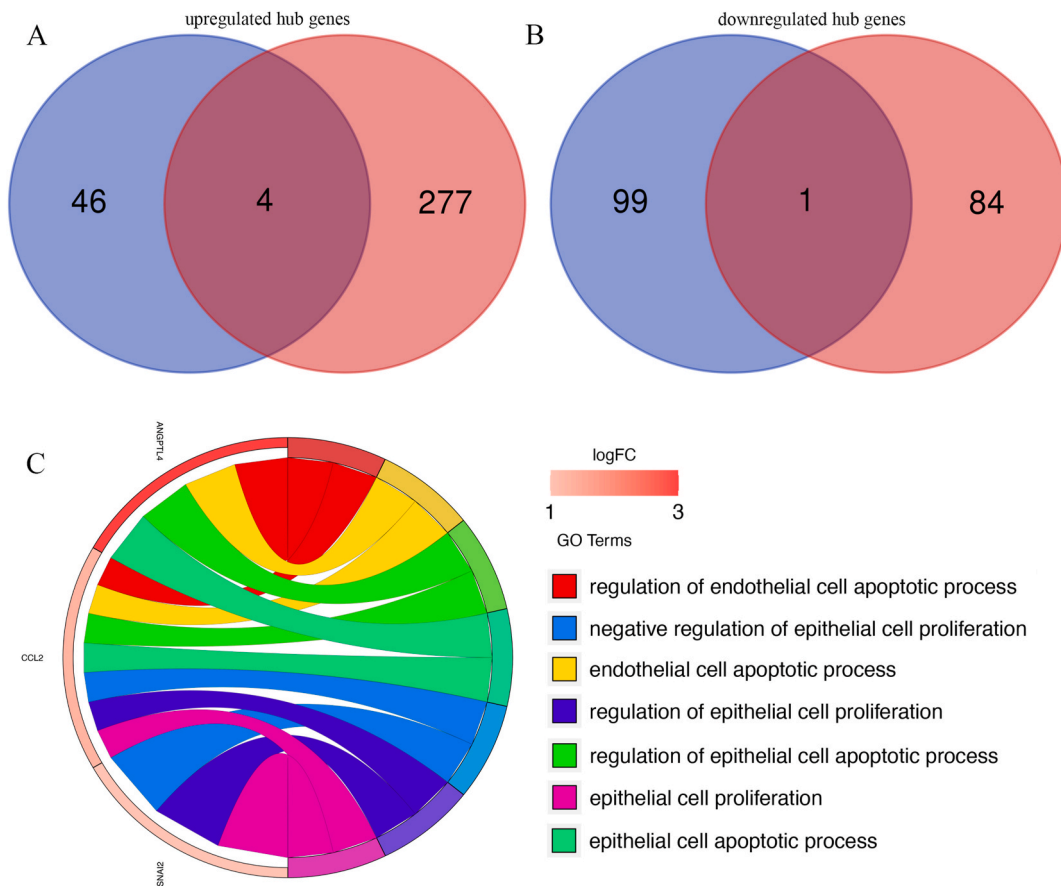


**Fig. 5.** Identification and enrichment analysis of the shear stress-associated hub DEGs in AD. (A) Four down-regulated hub DEGs after taking the intersection of DEGs in AD and shear stress-induced HAEC. (B) One up-regulated hub gene with common up-regulated expression in the three datasets after taking the intersection of DEGs in AD and shear stress-induced HAEC. (C) GO enrichment of shear stress-associated hub DEGs in AD. DEGs: differentially expressed genes.



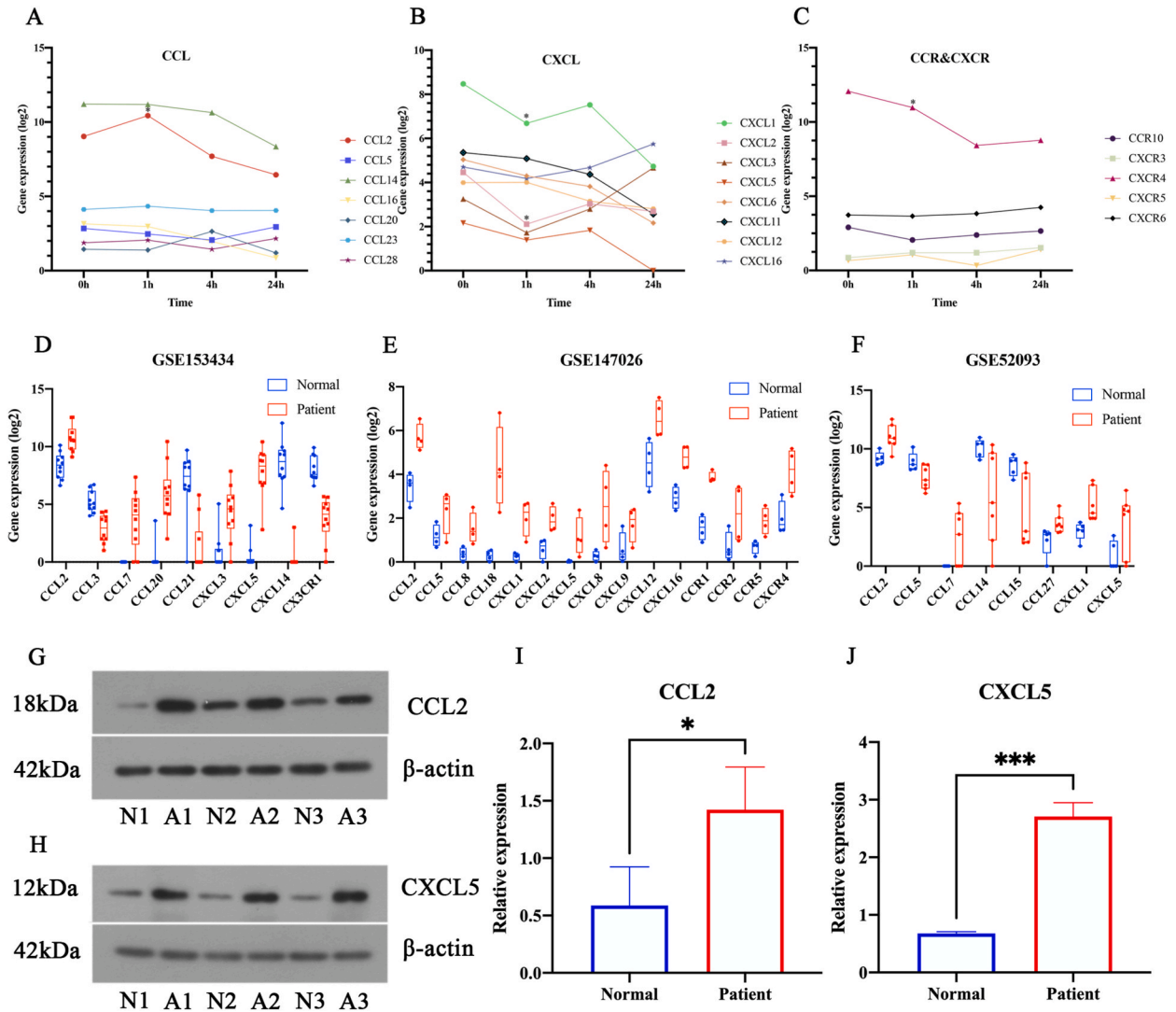


**Fig. 6.** Chemokine receptor and ligand profiles in pulsatile shear stress-induced HAEC and AD. (A–C) Trends of chemokine receptors and ligands change over time in shear stress-induced HAEC. (D–F) Significantly differently expressed chemokine receptors and ligands in three AD datasets. (G, H) Immunoblotting validation of chemokines CCL2 and CXCL5 is significantly differently expressed in the three AD datasets. (I, J) Quantitative data of relative protein level to  $\beta$ -actin. At least three experiments were repeated, and the representative figures are shown.  $*P < 0.05$ ,  $***P < 0.001$  compared with the control group. Before statistical comparisons, normality and equal variance were first tested. After checking for similar variance among normally distributed data, differences between the two groups were analyzed by Student’s *t*-test.

**Table 2**  
The details of the clinical tissue samples used for validation.

	Gender	Age	Hypertension	Smoking	Diabete	Source of Tissue Sample
A1	Male	50	Yes	Yes	No	Dissected ascending aorta obtained during surgery
A2	Male	55	Yes	Yes	No	Dissected ascending aorta obtained during surgery
A3	Male	46	Yes	Yes	No	Dissected ascending aorta obtained during surgery
N1	Male	49	Yes	Yes	No	Normal aortic tissue from heart transplantation donor due to cerebrovascular accident death
N2	Male	38	No	No	No	Normal aortic tissue from heart transplantation donor due to fall injury death
N3	Male	45	No	No	No	Normal aortic tissue from heart transplantation donor due to car accident death



important link in the occurrence and development of AD.

3.4. CCL2 and CXCL5 mediated immune cell infiltration in aortic dissection

Chemokines are central in the development and homeostasis of the immune system and are involved in protective or destructive immune and inflammatory responses [19]. Moreover, immune cell infiltration's role in AD has recently attracted increasing attention. This study aimed to determine the type of immune cell infiltration mediated by two core chemokines (CCL2 and CXCL5) that are significantly altered and involved in AD development.

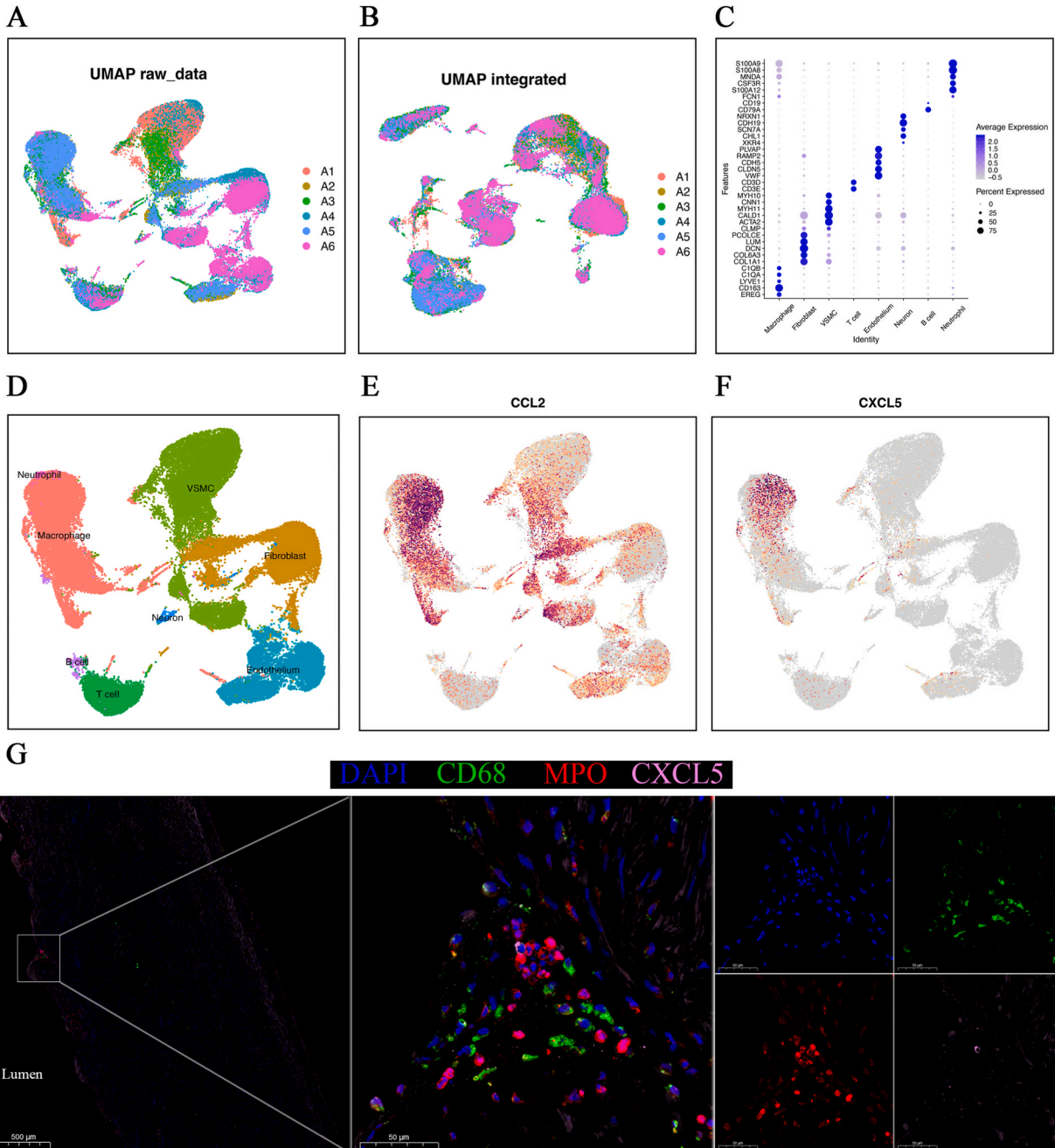


**Fig. 7.** Identifying CCL2 and CXCL5 origin by analyzing AD single-cell sequencing data and immunofluorescence. (A–B) Integration of six single-cell data done using the harmony package and the data before and after integration. (C) Detailed cell cluster annotations and information on marker genes. (D) Eight types of cell clusters identified from the aortic tissue of AD patients. (E–F) Featureplot of CCL2 and CXCL5. (G) Consistent localization of CD68 (a macrophage marker), MPO (a neutrophil marker), and CXCL5 in AD tissue.

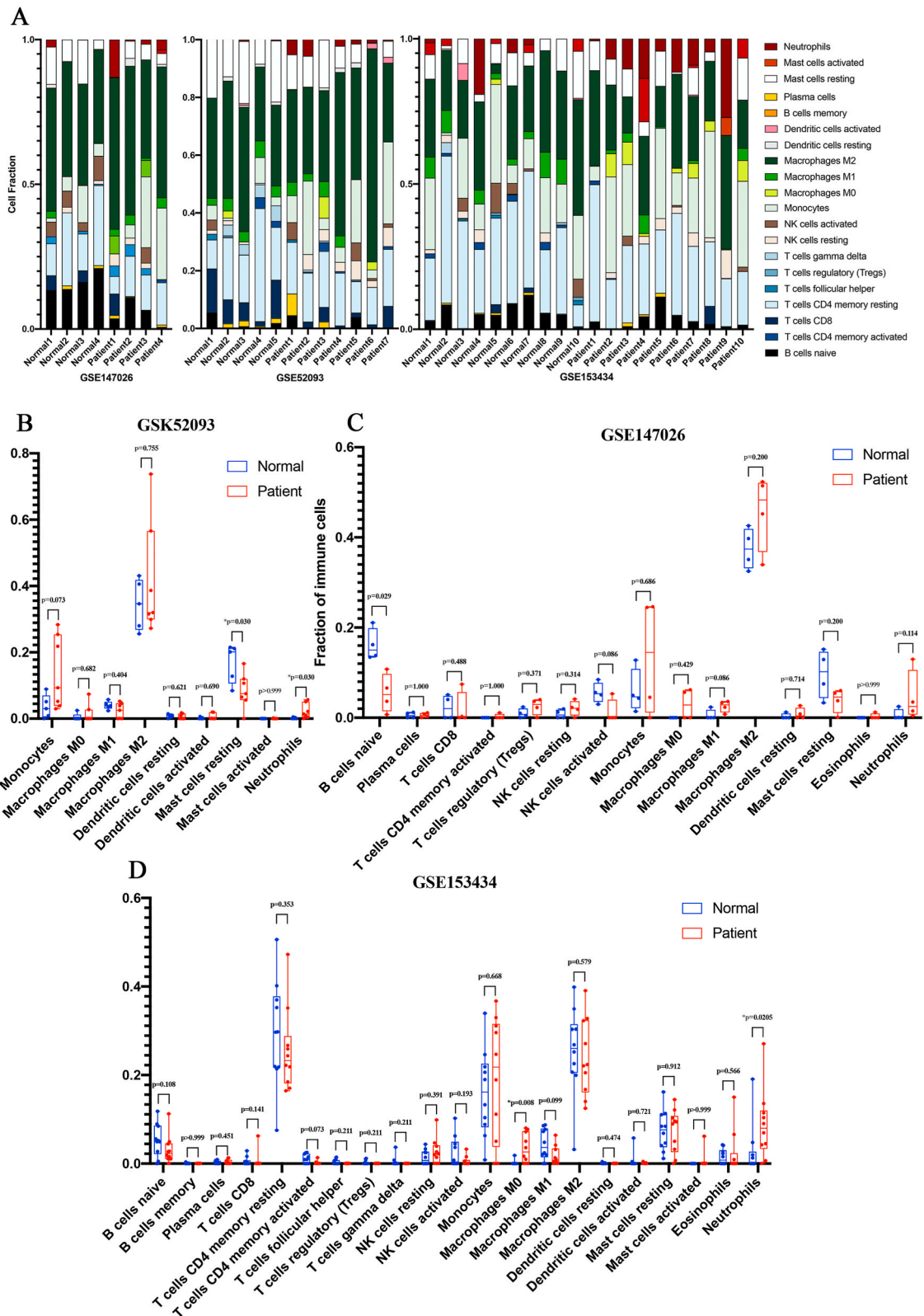


**Fig. 8.** Analysis of immune infiltration in the AD sets using CIBERSORTx. (A) Histogram of the fraction of 22 types of immune cells in each sample. (B–D) The percentage of immune cells in the AD sets was determined, and the Wilcoxon test was performed.

Furthermore, chemokines affect immune cell migration and activation by binding to receptors on the surface of immune cells, participating in the occurrence and development of diseases. Additionally, although we found that shear stress may induce CCL2 expression, CCL2 is expressed in many types of cells, including endothelium, epithelium, and bone marrow. Moreover, CCL2 strongly recruits monocytes, T lymphocytes, and natural killer cells [20] and activates these cells to stimulate the release of proinflammatory cytokines, such as interleukin (IL)-1, IL-6, and tumor necrosis factor- $\alpha$  [21]. However, CCL2 is a crucial regulator of monocyte trafficking, representing one of the strongest recruitment signals for monocytes to inflammation sites [22]. Furthermore, CXCL5 is a neutrophil chemoattractant whose concentration gradient determines neutrophil trafficking between blood and tissues [23]. Additionally, CXCL5 is expressed by many immune (macrophages and eosinophils) and non-immune cells (mesothelial cells and fibroblasts) [24]. To explore the origin of CCL2 and CXCL5 expressions, we selected the GSE213740 dataset of single-cell sequencing of AD samples from the GEO database for analysis. The dataset contained six AD samples. Six single-cell data were integrated using the harmony package, and the data before and after integration is visualized in Fig. 7A and B. For detailed cell cluster annotations and information on marker genes, see Fig. 7C. Moreover, eight types of cell clusters (endothelial cells, VSMCs, fibroblasts, macrophages, T cells, B cells, neutrophils, and some neuron cells) were identified from the aortic tissue of AD patients (Fig. 7D). Additionally, CCL2 was considered to have multiple origins, and CXCL5 was macrophage-derived (Fig. 7E and F). We further confirmed the above results using immunofluorescence, and the results showed consistent localization of macrophages (CD68), neutrophils (MPO), and CXCL5 in the aortic tissue of patients with AD (Fig. 7G). Furthermore, CIBERSORTx [15] was used to calculate the immune cell fraction in the normal tissues of patients with AD (Fig. 8A). We confirmed that the proportion of neutrophils in AD was significantly increased in GSE52093 and GSE153434. However, although an elevated trend was observed in GSE147026, the difference was not significant, probably due to the relatively small number of specimens (Fig. 8B–D). These results suggest neutrophils contribute significantly to AD, which is seldom reported in basic AD-related research.

#### 4. Discussion

AD is a life-threatening disease whose pathogenesis remains unclear. Although researchers have made some progress in actively developing AD models, it is still being determined why AD occurs only in specific aortic segments. The computational fluid dynamics-based study results suggest that the rupture positions corresponded to the area of maximum elevated wall shear stress in AD [6]. Notably, the role of biomechanics in AD goes beyond the fact that AD occurs when hemodynamic forces exceed the strength of the aortic wall, resulting in intimal tear and false lumen propagation. Exposure to specific flow patterns over time may change the structure of the aortic wall (remodeling), increasing the risk of degeneration and development of AD [25]. Therefore, considering the influence of shear stress will solve the problems encountered in existing studies.

First, common DEGs for AD were explored in a public database through bioinformatic analyses. We identified 150 AD hub genes and potential therapeutic agents for AD based on the common AD genes obtained above by cMAP. Although AD frequently has an acute onset and surgical treatment is the most common option for its management, in patients at high risk of AD, it is still necessary to find possible drugs to reduce the risk and postpone AD development. Next, through enrichment and PPI network analyses, we confirmed that the up-regulation of inflammation-related genes and down-regulation of VSMC-related genes are essential AD features and that CCL2 is a critical link. Moreover, we identified 366 shear stress-induced DEGs of HAEC in the GSE160611 dataset. Additionally, PROM1, ANGPTL4, SNAI2, CCL2, and GADD45B were identified as hub genes because of identical changes in their expression trends. Enrichment analysis showed they were related to endothelial apoptosis, suggesting that the induction of HAEC apoptosis and the simultaneous release of CCL2 are possible mechanisms underlying the involvement of shear stress in the pathophysiology of AD. It has been shown that inflamed endothelial cells can recruit monocytes by secreting CCL2 [26]. As confirmed by our bioinformatics results and previous studies [27], shear stress can lead to increased expression of CCL2 in vascular endothelial cells.

Previous studies have primarily focused on the role of smooth muscle cells and macrophages in AD, ignoring the role of HAEC in AD. However, Yang [28] recently reported that the disruption of endothelial tight junction function is an early event before AD formation, consistent with the findings of our study. Moreover, we found that the shear stress-induced increase in CCL2 expression occurs rapidly (within 1 h), and this response fades, falling below basal expression by 4 h and continuing to decline until 24 h. This suggests that shear stress-induced production of CCL2 by HAEC may be an early pathophysiological process in AD. This phenomenon has been confirmed in previous studies [29] and partly explains why high blood pressure variability is a risk factor for AD rather than high blood pressure. High blood pressure variability may lead to frequent changes in shear stress, possibly inducing more CCL2 secretion by endothelial cells and, consequently, more local recruitment of monocytes. Furthermore, we found that oscillatory shear stress did not increase CCL2 gene expression compared with pulsatile shear stress (Fig. S2), which supports our hypothesis to some extent. Lastly, pulsatile stress is mainly observed in straight arterial segments, while oscillatory shear is observed primarily in the aortic branches [18]; thus, the shear stress in the aorta is mainly pulsatile.

Several studies have demonstrated the high expression of CCL2 in animal models of AD [30,31]. Similarly, our study confirmed the highly increased expression of CCL2 in human AD tissues. Notably, although shear stress-induced production of CCL2 by endothelial cells is the initiating link in AD, endothelial cells do not exclusively secrete CCL2 during the pathophysiology of AD, as the shear stress-induced secretion of CCL2 by endothelial cells is transient. Moreover, our analysis of single-cell sequencing data from AD tissues confirmed that CCL2 is derived from macrophages, smooth muscle cells, and fibroblasts and that its expression in these cells is significantly higher than in endothelial cells. Therefore, we hypothesized that when shear stress-induced CCL2 secretion locally recruits monocytes/macrophages from HAEC, the local microenvironment may provide suitable monocyte/macrophage activation conditions. Additionally, the interaction of activated monocytes/macrophages with fibroblasts, smooth muscle cells, and the extracellular matrix may increase local cell secretion of CCL2, leading to a cascade amplification effect of local inflammation, ultimately

leading to the onset of AD.

Besides CCL2, CXCL5 was the only chemokine with elevated expression in all three AD datasets. Additionally, we verified high CXCL5 protein levels in human AD tissue. However, its role in AD is less studied. Chang et al. [32] reported that CXCL5 inhibition reduced neutrophil infiltration and MMP9 expression, thereby reducing the incidence of AD, which coincides with CXCL5's role as a strong chemotactic factor for neutrophils. Therefore, the high expression of CXCL5 in AD signifies that neutrophils may play a vital role in AD. However, the role of neutrophils in AD pathophysiology has received far less attention than monocytes/macrophages. The prevalence of elevated neutrophils has been demonstrated in blood tests of patients with AD, which may predict poor prognosis [33]. Additionally, local neutrophil recruitment and activation reportedly mediate aortic dilation and rupture in AD [34], besides the possible involvement of neutrophils in AD development through the secretion of MMP9 [7]. Moreover, it has been suggested that MMP9 and macrophage distribution are spatially compatible in AD, and macrophages can direct T lymphocytes and neutrophils to the lesion area and regulate the vascular remodeling pathway, confirmed by the targeted knockdown of monocytes/macrophages using LYSM<sup>IDTR</sup> mice [35]. Additionally, we demonstrated that CXCL5 is mainly macrophage-derived by analyzing single-cell sequencing data and immunofluorescence. Therefore, we believe macrophages can secrete CXCL5 in AD and recruit neutrophils after local macrophage recruitment and activation, which are essential aspects of AD, although previously neglected. Overall, we have a basic understanding of the possible mechanism of shear stress involvement in AD. In summary, shear stress leads to endothelial cell damage, apoptosis, and CCL2 expression, followed by the local recruitment and activation of monocytes/macrophages, which secrete CXCL5 to recruit neutrophils. Next, the neutrophils act on the local cells and extracellular matrix, leading to AD. The hemodynamic characteristics of the aorta make it more susceptible to the above processes in specific areas with high variation in shear stress. Therefore, AD occurs in specific areas, indicating the certainty of the contingency in AD. Thus, neutralizing the chemokines CCL2 and CXCL5 by using specific monoclonal antibodies to block their modulation of the "endothelial-macrophage-neutrophil" axis may be an additional strategy to postpone AD progression. Medicines now available targeting CCL2-CCR2 are listed as follows. Carlumab (CNTO 888) is a high-affinity monoclonal antibody targeting specifically CCL2, initially considered for treating solid tumors [36]. Still, it failed to influence response rates and was discontinued despite showing potent therapeutic efficacy in preclinical mouse models. In addition, BMS-813160 is another small molecule compound that targets CCR2 as a dual antagonist of CCR2 and CCR5 [37]. However, no clinical trials or applications have yet been conducted. For CXCL5-CXCR2, there is still no relevant pharmaceutical product available. Could the available drugs targeting CCL2-CCR2 possibly contribute to preventing and treating AD? Or is it possible to develop drugs to prevent and treat AD targeting CXCL5-CXCR2? However, there is relatively little existing research on CCL2 and CXCL5 action mechanisms in AD, and there are also fewer available clinical drugs based on the targeting of CCL2 and CXCL5 and their receptors, so further research is needed. We still have a long way to go.

Our study has some limitations. First, the integration of multiple datasets and reliance on public databases may introduce inherent biases or confounders. Second, although we have proposed the existing hypothesis through the analysis of various types of bioinformatics data and the validation of clinical tissue specimens, the results would be more convincing if corroborated with the results of animal experiments. Third, besides the effect of shear stress on endothelial cells, shear stress may affect the function of VSMCs, fibroblasts, and other types of cells, which needs further study.

## 5. Conclusions

Through integrative analysis, we elucidated that shear stress may induce apoptosis of endothelial cells and release of CCL2, which in turn leads to local monocyte/macrophage recruitment, and the local microenvironment may lead to macrophage activation and secretion of CXCL5, as well as neutrophil recruitment, ultimately leading to AD. In summary, the chemokine CCL2 and CXCL5-mediated "Endothelial-Monocyte-Neutrophil" axis may contribute to the development of shear stress-induced AD. These findings provide possible therapeutic targets and drugs for preventing and treating AD, and our study offers potential insights for drug development in AD.

## Ethics approval and consent to participate

The study was approved by the Ethics Committee of Xijing Hospital of the Fourth Military Medical University (No.20120216).

## Funding

This work was supported by the National Natural Science Foundation of China (grant nos. 82070503, 82270420, and 82241204), Key R&D Program of Shaanxi Province, China (2022ZDLSF02-01), Innovation Capability Support Program of Shaanxi Province, China (2021 PT-019), and Natural Science Foundation of Shaanxi Province, China (2021JQ-347).

## Data availability statement

The datasets analyzed during this study are available at <http://www.ncbi.nlm.nih.gov/geo/accession> number:(GSE147206, GSE153434, GSE52093, GSE160611, and GSE213740). In addition, on reasonable request, the corresponding author will provide all the data and R script used in this study.



## CRediT authorship contribution statement

**Chao Xue:** Writing – original draft. **Liqing Jiang:** Validation. **Bin Zhang:** Validation. **Jingwei Sun:** Resources. **Hanzhao Zhu:** Conceptualization, Resources. **Linhe Lu:** Resources. **Liyun Zhang:** Resources. **Bo Yu:** Resources. **Weiguang Wang:** Resources. **Bo Xu:** Resources. **Zhenxiao Jin:** Resources. **Shiqiang Yu:** Resources. **Jincheng Liu:** Conceptualization. **Kai Ren:** Conceptualization. **Weixun Duan:** Conceptualization, Funding acquisition, Project administration.

## Declaration of competing interest

The authors declare that they have no known competing financial interests or personal relationships that could have appeared to influence the work reported in this paper.

## Appendix A. Supplementary data

Supplementary data to this article can be found online at <https://doi.org/10.1016/j.heliyon.2023.e23312>.

## References

- [1] M. Silaschi, J. Byrne, O. Wendler, Aortic dissection: medical, interventional and surgical management, *Heart* 103 (1) (2017) 78–87.
- [2] L. Xia, C. Sun, H. Zhu, M. Zhai, L. Zhang, L. Jiang, P. Hou, J. Li, K. Li, Z. Liu, et al., Melatonin protects against thoracic aortic aneurysm and dissection through SIRT1-dependent regulation of oxidative stress and vascular smooth muscle cell loss, *J. Pineal Res.* 69 (1) (2020), e12661.
- [3] J. Dong, S. Li, Z. Lu, P. Du, G. Liu, M. Li, C. Ma, J. Zhou, J. Bao, HCMV-miR-US33-5p promotes apoptosis of aortic vascular smooth muscle cells by targeting EPAS1/SLC3A2 pathway, *Cell. Mol. Biol. Lett.* 27 (1) (2022) 40.
- [4] K. Yang, J. Ren, X. Li, Z. Wang, L. Xue, S. Cui, W. Sang, T. Xu, J. Zhang, J. Yu, et al., Prevention of aortic dissection and aneurysm via an ALDH2-mediated switch in vascular smooth muscle cell phenotype, *Eur. Heart J.* 41 (26) (2020) 2442–2453.
- [5] X. Wang, H. Zhang, L. Cao, Y. He, A. Ma, W. Guo, The role of macrophages in aortic dissection, *Front. Physiol.* 11 (2020) 54.
- [6] Q. Chi, Y. He, Y. Luan, K. Qin, L. Mu, Numerical analysis of wall shear stress in ascending aorta before tearing in type A aortic dissection, *Comput. Biol. Med.* 89 (2017) 236–247.
- [7] T. Kurihara, R. Shimizu-Hirota, M. Shimoda, T. Adachi, H. Shimizu, S.J. Weiss, H. Itoh, S. Hori, N. Aikawa, Y. Okada, Neutrophil-derived matrix metalloproteinase 9 triggers acute aortic dissection, *Circulation* 126 (25) (2012) 3070–3080.
- [8] X. Zhou, Z. Chen, J. Zhou, Y. Liu, R. Fan, T. Sun, Transcriptome and N6-methyladenosine RNA methylome analyses in aortic dissection and normal human aorta, *Front Cardiovasc Med* 8 (2021), 627380.
- [9] Z. Zhou, Y. Liu, X. Zhu, X. Tang, Y. Wang, J. Wang, C. Xu, D. Wang, J. Du, Q. Zhou, Exaggerated autophagy in stanford type A aortic dissection: a transcriptome pilot analysis of human ascending aortic tissues, *Genes* 11 (10) (2020).
- [10] S. Pan, D. Wu, A.E. Teschendorff, T. Hong, L. Wang, M. Qian, C. Wang, X. Wang, JAK2-centered interactome hotspot identified by an integrative network algorithm in acute Stanford type A aortic dissection, *PLoS One* 9 (2) (2014), e89406.
- [11] B. Zhang, K. Zeng, R.C. Guan, H.Q. Jiang, Y.J. Qiang, Q. Zhang, M. Yang, B.P. Deng, Y.Q. Yang, Single-cell RNA-seq analysis reveals macrophages are involved in the pathogenesis of human sporadic acute type A aortic dissection, *Biomolecules* 13 (2) (2023) 399.
- [12] Y. Zhou, B. Zhou, L. Pache, M. Chang, A.H. Khodabakhshi, O. Tanaseichuk, C. Benner, S.K. Chanda, Metascape provides a biologist-oriented resource for the analysis of systems-level datasets, *Nat. Commun.* 10 (1) (2019) 1523.
- [13] W. Walter, F. Sánchez-Cabo, M. Ricote, GPlot: an R package for visually combining expression data with functional analysis, *Bioinformatics* 31 (17) (2015) 2912–2914.
- [14] J. Lamb, The Connectivity Map: a new tool for biomedical research, *Nat. Rev. Cancer* 7 (1) (2007) 54–60.
- [15] A.M. Newman, C.B. Steen, C.L. Liu, A.J. Gentles, A.A. Chaudhuri, F. Scherer, M.S. Khodadoust, M.S. Esfahani, B.A. Luca, D. Steiner, et al., Determining cell type abundance and expression from bulk tissues with digital cytometry, *Nat. Biotechnol.* 37 (7) (2019) 773–782.
- [16] T. Stuart, A. Butler, P. Hoffman, C. Hafemeister, E. Papalexi, W.M. Mauck 3rd, Y. Hao, M. Stoeckius, P. Smibert, R. Satija, Comprehensive integration of single-cell data, *Cell* 177 (7) (2019), 1888–902.e21.
- [17] X. Bao, C. Lu, J.A. Frangos, Temporal gradient in shear but not steady shear stress induces PDGF-A and MCP-1 expression in endothelial cells: role of NO, NF kappa B, and egr-1, *Arterioscler. Thromb. Vasc. Biol.* 19 (4) (1999) 996–1003.
- [18] M.R. Maurya, S. Gupta, J.Y. Li, N.E. Ajami, Z.B. Chen, J.Y. Shyy, S. Chien, S. Subramaniam, Longitudinal shear stress response in human endothelial cells to atheroprotective and atheroprotective conditions, *Proc Natl Acad Sci U S A* 118 (4) (2021).
- [19] C.E. Hughes, R.J.B. Nibbs, A guide to chemokines and their receptors, *FEBS J.* 285 (16) (2018) 2944–2971.
- [20] G. Lazennec, A. Richmond, Chemokines and chemokine receptors: new insights into cancer-related inflammation, *Trends Mol. Med.* 16 (3) (2010) 133–144.
- [21] S. Kadomoto, K. Izumi, A. Mizokami, Roles of CCL2-CCR2 Axis in the tumor microenvironment, *Int. J. Mol. Sci.* 22 (16) (2021) 8530.
- [22] M.K. Georgakias, J. Bernhagen, L.H. Heitman, C. Weber, M. Dichgans, Targeting the CCL2-CCR2 axis for atheroprotection, *Eur. Heart J.* 43 (19) (2022) 1799–1808.
- [23] R. Phillips, CXCL5 effective in mouse model of SLE, *Nat. Rev. Rheumatol.* 18 (12) (2022) 673.
- [24] W. Zhang, H. Wang, M. Sun, X. Deng, X. Wu, Y. Ma, M. Li, S.M. Shuoa, Q. You, L. Miao, CXCL5/CXCR2 axis in tumor microenvironment as potential diagnostic biomarker and therapeutic target, *Cancer Commun.* 40 (2–3) (2020) 69–80.
- [25] M.Y. Salmasi, S. Pirola, S. Sasidharan, S.M. Fisichella, A. Redaelli, O.A. Jarral, D.P. O'Regan, A.Y. Oo, J.E. Moore Jr., X.Y. Xu, T. Athanasiou, High wall shear stress can predict wall degradation in ascending aortic aneurysms: an integrated biomechanics study, *Front. Bioeng. Biotechnol.* 9 (2021), 750656.
- [26] U. Maus, S. Henning, H. Wenschuh, K. Mayer, W. Seeger, J. Lohmeyer, Role of endothelial MCP-1 in monocyte adhesion to inflamed human endothelium under physiological flow, *Am. J. Physiol. Heart Circ. Physiol.* 283 (6) (2002) H2584–H2591.
- [27] C. Chu, G. Xu, X. Li, Z. Duan, L. Tao, H. Cai, M. Yang, X. Zhang, B. Chen, Y. Zheng, et al., Sustained expression of MCP-1 induced low wall shear stress loading in conjunction with turbulent flow on endothelial cells of intracranial aneurysm, *J. Cell Mol. Med.* 25 (1) (2021) 110–119.
- [28] X. Yang, C. Xu, F. Yao, Q. Ding, H. Liu, C. Luo, D. Wang, J. Huang, Z. Li, Y. Shen, et al., Targeting endothelial tight junctions to predict and protect thoracic aortic aneurysm and dissection, *Eur. Heart J.* 44 (14) (2023).
- [29] J. Zhou, Y.S. Li, S. Chien, Shear stress-initiated signaling and its regulation of endothelial function, *Arterioscler. Thromb. Vasc. Biol.* 34 (10) (2014) 2191–2198.
- [30] X. Ju, T. Ijaz, H. Sun, S. Ray, W. Lejeune, C. Lee, A. Recinos 3rd, D.C. Guo, D.M. Milewicz, R.G. Tilton, A.R. Brasier, Interleukin-6-signal transducer and activator of transcription-3 signaling mediates aortic dissections induced by angiotensin II via the T-helper lymphocyte 17-interleukin 17 axis in C57BL/6 mice, *Arterioscler. Thromb. Vasc. Biol.* 33 (7) (2013) 1612–1621.



- [31] B.C. Tieu, C. Lee, H. Sun, W. Lejeune, A. Recinos 3rd, X. Ju, H. Spratt, D.C. Guo, D. Milewicz, R.G. Tilton, A.R. Brasier, An adventitial IL-6/MCP1 amplification loop accelerates macrophage-mediated vascular inflammation leading to aortic dissection in mice, *J. Clin. Invest.* 119 (12) (2009) 3637–3651.
- [32] T.T. Chang, L.Y. Liao, J.W. Chen, Inhibition on CXCL5 reduces aortic matrix metalloproteinase 9 expression and protects against acute aortic dissection, *Vascul Pharmacol* 141 (2021), 106926.
- [33] E. Sbarouni, P. Georgiadou, A. Analitis, V. Voudris, High neutrophil to lymphocyte ratio in type A acute aortic dissection facilitates diagnosis and predicts worse outcome, *Expert Rev. Mol. Diagn* 15 (7) (2015) 965–970.
- [34] A. Anzai, M. Shimoda, J. Endo, T. Kohno, Y. Katsumata, T. Matsuhashi, T. Yamamoto, K. Ito, X. Yan, K. Shirakawa, et al., Adventitial CXCL1/G-CSF expression in response to acute aortic dissection triggers local neutrophil recruitment and activation leading to aortic rupture, *Circ. Res.* 116 (4) (2015) 612–623.
- [35] X. Li, D. Liu, L. Zhao, L. Wang, Y. Li, K. Cho, C. Tao, B. Jiang, Targeted depletion of monocyte/macrophage suppresses aortic dissection with the spatial regulation of MMP-9 in the aorta, *Life Sci.* 254 (2020), 116927.
- [36] G. Obmolova, A. Teplyakov, T.J. Malia, T.L. Grygiel, R. Sweet, L.A. Snyder, G.L. Gilliland, Structural basis for high selectivity of anti-CCL2 neutralizing antibody CNTO 888, *Mol. Immunol.* 51 (2) (2012) 227–233.
- [37] R.J. Cherney, P. Anjanappa, K. Selvakumar, D.G. Batt, G.D. Brown, A.V. Rose, R. Vuppugalla, J. Chen, J. Pang, S. Xu, et al., BMS-813160: a potent CCR2 and CCR5 dual antagonist selected as a clinical candidate, *ACS Med. Chem. Lett.* 12 (11) (2021) 1753–1758.